



# 1 Measurement report: Determination of Black Carbon concentration 2 in PM<sub>2.5</sub> fraction by Multi-wavelength absorption black carbon 3 instrument (MABI)

4 Anna Rys<sup>1</sup>, Lucyna Samek<sup>1</sup>

5 <sup>1</sup>Faculty of Physics and Applied Computer Science, AGH University of Science and Technology, 30 Mickiewicza Ave,  
6 Krakow, 30-059, Poland

7 *Correspondence to:* Lucyna Samek (lucyna.samek@fis.agh.edu.pl)

8 **Abstract.** The evaluation of black carbon (BC) sources is very important, especially in environmental sciences. This study  
9 shows how the contributions of biomass burning and fossil fuel/traffic to PM<sub>2.5</sub> mass can be assessed. MABI was used for this  
10 purpose and gave the possibility to measure the transmission of light at different wavelengths. Absorption coefficients were  
11 calculated from measurements data and recalculated for concentrations of eBC. The samples of PM<sub>2.5</sub> fraction were collected  
12 from February 1, 2020 to March 27, 2021 every third day in Krakow, Poland (50°04'N, 19°54'47" E). The concentrations of  
13 equivalent BC (eBC) from fossil fuel/traffic and biomass burning were in the range 0.82-11.64  $\mu\text{g m}^{-3}$  and 0.007-0.84  
14  $\mu\text{g m}^{-3}$ , respectively. At the same time, PM<sub>2.5</sub> concentrations varied from 3.14 to 55.24  $\mu\text{g m}^{-3}$ . It means that about 18 % of  
15 PM<sub>2.5</sub> mass belongs to eBC and 11.3 % of this value comes from biomass burning. The eBC contribution is the significant part  
16 of PM<sub>2.5</sub> mass and we observed seasonal variation of the eBC concentration during the year with the peak in winter. The  
17 contribution of biomass burning to PM<sub>2.5</sub> mass is more stable during the whole year. The eBC concentration during workdays  
18 is a bit higher than during weekend days but biomass burning is similar for both days (work and weekend taken as the mean  
19 for the whole period).

## 20 1 Introduction

21 For many years, scientists have conducted air pollution research that led to the possibility of successful identification of  
22 numerous aerosol particular matter (PM) components harmful to the environment and as such to human health. Now, scientists  
23 can perform a quantitative and qualitative analysis of components present in the air as organic and inorganic substances,  
24 chemical elements, heavy metals, and black carbon.

25 The largest contributor to air pollution and global change is the emission of the carbonaceous particle which is produced during  
26 the combustion of biomass and fossil fuel (Petzold et al., 2013). Black carbon (BC) is the one fraction of the carbonaceous  
27 aerosol which is produced during incomplete combustion (Diapouli et al., 2017; European Environment Agency, 2013; Petzold  
28 et al., 2013). BC is characterized by the strong absorbs of all wavelengths of solar radiation (Bond and Bergstrom, 2006;  
29 Petzold et al., 2013; U.S. EPA (U.S. Environmental Protection Agency), 2012). Based on the fact that light absorption particles



30 can warm the atmosphere, scientists consider the BC as the second most critical reason for global warming in terms of direct  
31 impact (Jacobson, 2001; Liu et al., 2016). The BC influences not only general climate change but also causes indirect effects  
32 for instance it reduces local visibility and is responsible for the appearance of the brown hazes in a city (Horvath, 1993; U.S.  
33 EPA (U.S. Environmental Protection Agency), 2012). According to the “Report to Congress on Black Carbon”, most of the  
34 global BC emissions come from Asia, Latin America, and Africa while major sources were open biomass burning, residential,  
35 and transport (U.S. EPA (U.S. Environmental Protection Agency), 2012). Although BC has a strong harmful impact on the  
36 environment, the lifetime of BC in the atmosphere is relatively short. The reduction of the BC can be achieved by the strategies  
37 targeting to lower BC emissions connection with the identified sources of BC, global air pollution management, and policy-  
38 making (Diapouli et al., 2017; U.S. EPA (U.S. Environmental Protection Agency), 2012). Since research on black carbon is  
39 being constantly improved there is some inconsistency in terminology. Bond and Bergstrom indicated that scientists use  
40 different names for “Black Carbon” for instance: “soot”, “light absorbing carbon”, “elemental carbon”, “refractory carbon”,  
41 “graphitic carbon” (Bond and Bergstrom, 2006; Petzold et al., 2013). These nomenclatures are connected with composition,  
42 optical properties, and particle morphology.

43 Over the years, different measurement techniques and instruments were used to describe and determine the BC mass. These  
44 techniques are usually based on light absorption scattering or thermal radiation measurements. The instruments which are  
45 commonly used range from the aethalometer to Multi-angle absorption photometry (MAAP) or Photoacoustic Instruments, as  
46 well as techniques, and recommended terminology that is widely discussed in review papers by Petzold, A. et al, Bond, T. C.  
47 & Bergstrom, R., and Lack, D. et al (Bond and Bergstrom, 2006; Lack et al., 2013; Petzold et al., 2013; Petzold and  
48 Schönlinner, 2004).

49 There are a lot of publications about BC and most of them analyzed fraction  $PM_{2.5}$ . What is more, the Report EU presented  
50 results of BC analysis of other countries based on fraction  $PM_{2.5}$ . This study was also conducted basing on the BC from fraction  
51  $PM_{2.5}$  enabling comparison of received results with previously presented studies.

52 Our study aims to analyze the results of light absorption coefficients and BC mass concentrations which were obtained for  
53 different wavelengths. The calculation is based on the Lambert-Beer law, where  $\sigma_a$  is the absorption coefficients of the aerosol  
54 particles:

$$55 \frac{I_0}{I} = \exp(\sigma_a * X), \quad (1)$$

56 where  $I_0$  and  $I$  are the unexposed intensity and the exposed transmission intensity,  $X$  is the length of the sampled air column  
57 (Taha et al., 2007a).

58 This paper describes the methodology of calculating the results obtained by MABI step by step. Next, the results are  
59 demonstrated like graphs and tables. The key aspect is legislative changes which are in force in Kraków which should have an  
60 immense impact. Our measurement was conducting after that the local government implemented the ban on using solid fuel  
61 in households stoves in September 2019 in Krakow. We are convinced, that to compare previous studies  
62 (<https://acp.copernicus.org/preprints/acp-2021-197/>), our study is very valuable and it demonstrates current situation under



63 new circumstances. Our paper presents the most recent data, which last record was from March this year. What is more, our  
64 manuscript especially concentrations on presenting clearly data for BC of fraction  $PM_{2.5}$ .  
65 To the best of our knowledge, this is one of the first studies which includes the results of measurement by MABI for the whole  
66 year. Therefore we were not able to compare our results presented in this paper with the results from similar studies carried  
67 out by this instrument. However, we believe that our work will be valuable for organizations and institutes which have just  
68 started or continue working with MABI for the comparison or verification of the results.

## 69 **2 Sampling and Method**

### 70 **2.1 Sampling location**

71 The sampling camping was conducted from the research station located at AGH University of Science and Technology in  
72 Krakow (50°04'00.5" N, 19°54'46.8" E). This station is equivalent to the urban background station. Next to the sampling place,  
73 there are housing estates and a two-lane dual carriageway. The sampling place is about 2 km from City Center.

### 74 **2.2 Sampling**

75 Sampling was performed between February 1, 2020, and March 27, 2021 for 24 hours every three days. Some of the sampling  
76 days were omitted due to the temporary suspension of the research.  $PM_{2.5}$  samples were collected on Teflon filters (GE's  
77 Whatman, PTFE 46.2 mm, 2.0  $\mu\text{m}$ ), by the use of a low-volume ( $2.3 \text{ m}^3 \text{ h}^{-1}$ ) sampler (Sequential 47/50-CD with Peltier  
78 cooler, Sven Leckel GmbH, Berlin, Germany). The concentration of the fine fraction was determined. The mass of filters was  
79 measured before and after sampling. The filters were stored in the following condition  $20 \pm 1 \text{ }^\circ\text{C}$  and humidity  $50 \pm 5 \%$  for 24  
80 hours before weighing. The Teflon filters were analyzed for black carbon by MABI.

### 81 **2.3 Multi-wavelength absorption black carbon instrument**

82 Multi-wavelength absorption black carbon instrument (MABI) measures light absorption at seven different wavelengths: 405  
83 nm(UV), 465 nm, 525 nm, 639 nm, and infrared 870 nm, 940 nm, and 1050 nm. MABI was developed by the Australian  
84 Nuclear Science and Technology Organisation ([www.ansto.gov.au](http://www.ansto.gov.au)). This instrument consists of the optical assembly and  
85 electronic case. The instrument optics includes, among others, the multi-wavelength light source  
86 (7 LEDs), sampler holder, and photo-detector. What is more, it is used the opaque glass in "MABI units to scatter the scattered  
87 light back through the filter to the detector"(David D. Cohen, 2020). The calibration, zero the detector is performed  
88 automatically and saved by the MABI software application. All results are saved by the MABI software application as a ".csv".  
89 Data analysis was performed using Excel.  
90 The samples were scanned before and after sampling by MABI. MABI scans were performed on unexposed filters to determine  
91 the absorption at each wavelength from the filter substrate and obtained data is called  $I_0$ . Scans were repeated on the same filter



92 after sampling (exposed filters) to determine the absorption at each wavelength from filter substrate and collection particles  
93 and this data is called  $I$ . Based on these values ( $I_0$  and  $I$ ), the exposed filter area and sampled air volume, the black carbon light  
94 absorption coefficients  $b_{abs}$  ( $Mm^{-1}$ ) were determined at each wavelength with the following equation:

$$95 \quad b_{abs} = 10^2 \cdot \frac{A}{V} \cdot \ln \left[ \frac{I_0}{I} \right], \quad (2)$$

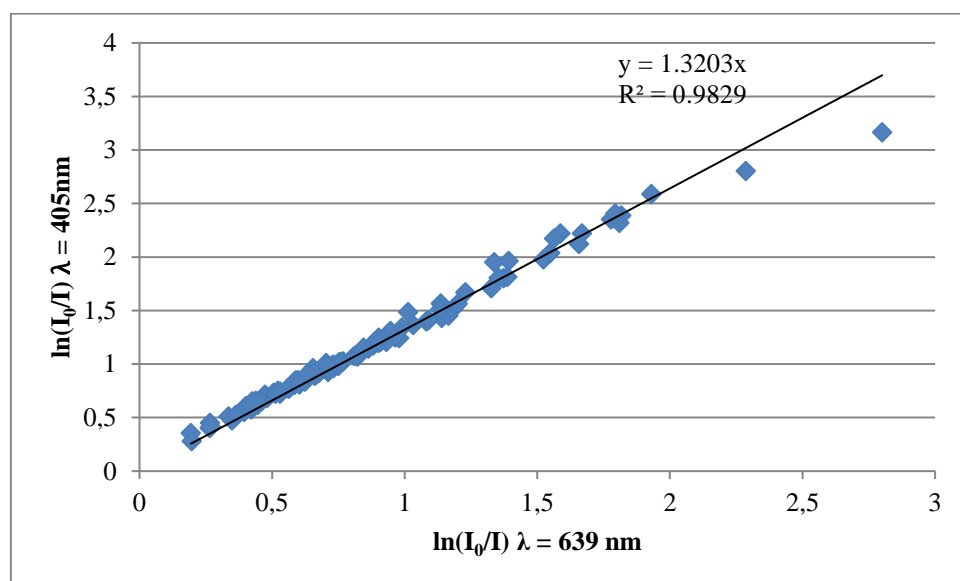
96 here  $I_0$  and  $I$  are the light transmission through an unexposed filter and an exposed filter. Parameter  $A$  is the collection area of  
97 the exposed filter ( $cm^2$ ) and  $V$  is the volume of sampled air on the filter ( $m^3$ ).

98 The black carbon (BC) mass concentration ( $ngm^{-3}$ ) was obtained using a mass absorption coefficient  $\varepsilon$  ( $m^2g^{-1}$ ) at each  
99 wavelength from:

$$100 \quad BC \text{ (} ngm^{-3} \text{)} = \frac{10^5 \cdot A}{\varepsilon \cdot V} \cdot \ln \left[ \frac{I_0}{I} \right] = \frac{10^3 \cdot b_{abs}}{\varepsilon}, \quad (3)$$

101 MABI Manual presents tests, results and mass absorption coefficients for different types of filters. Following the study  
102 presented by Atanacio et al., David D. Cohen, Taha et al (Atanacio et al., n.d.; David D. Cohen, 2020; Taha et al., 2007b), the  
103 Equation (3) was presented below and the values mass absorption coefficient  $\varepsilon$  for  $\lambda = 639$  nm was assumed as  $\varepsilon_{\lambda=639 \text{ nm}} =$   
104  $6.036 m^2 g^{-1}$ , which was recommended for 47mm Teflon filters by ANSTO. The author assumed scattering correction (C)  
105 and loading correction (R) based on the deep discussion presented in (David D. Cohen, 2020), where C and R (C = R = 1).  
106 The mass absorptions coefficients, for each wavelength, was estimated using the following calculation formulas, where  $\lambda_2 =$   
107  $\lambda_{639 \text{ nm}}$ ,

$$108 \quad \varepsilon(\lambda_1) = \varepsilon(\lambda_2) \cdot \text{gradient} \left( \frac{\lambda_2}{\lambda_1} \right) \quad (4)$$



109  
110 **Figure 1** The plot of  $\ln(I_0/I)$  for  $\lambda = 405$ nm versus  $\ln(I_0/I)$  for  $\lambda = 639$  nm, where  $\text{gradient} \left( \frac{\lambda_2}{\lambda_1} \right) = 1.3203$ , and  $\varepsilon(\lambda_{405}) =$   
111  $7.97m^2g^{-1}$  for sampling from Krakow site.

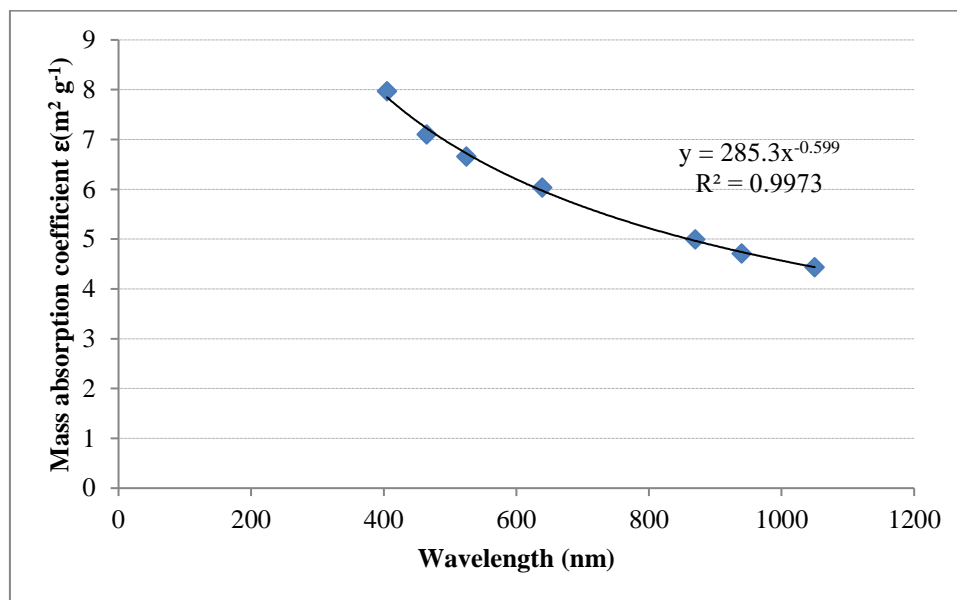


### 112 3 Results and discussion

113 The raw data obtained by MABI were calculated according to the methodology described above and were transformed to  
114 absorption coefficients ( $\epsilon$ ), equivalent black carbon (eBC) mass concentrations. The mass absorption coefficient for  
115 wavelength is presented as:

$$116 \quad \epsilon(\lambda) = a \cdot \lambda^{-\alpha}, \quad (2)$$

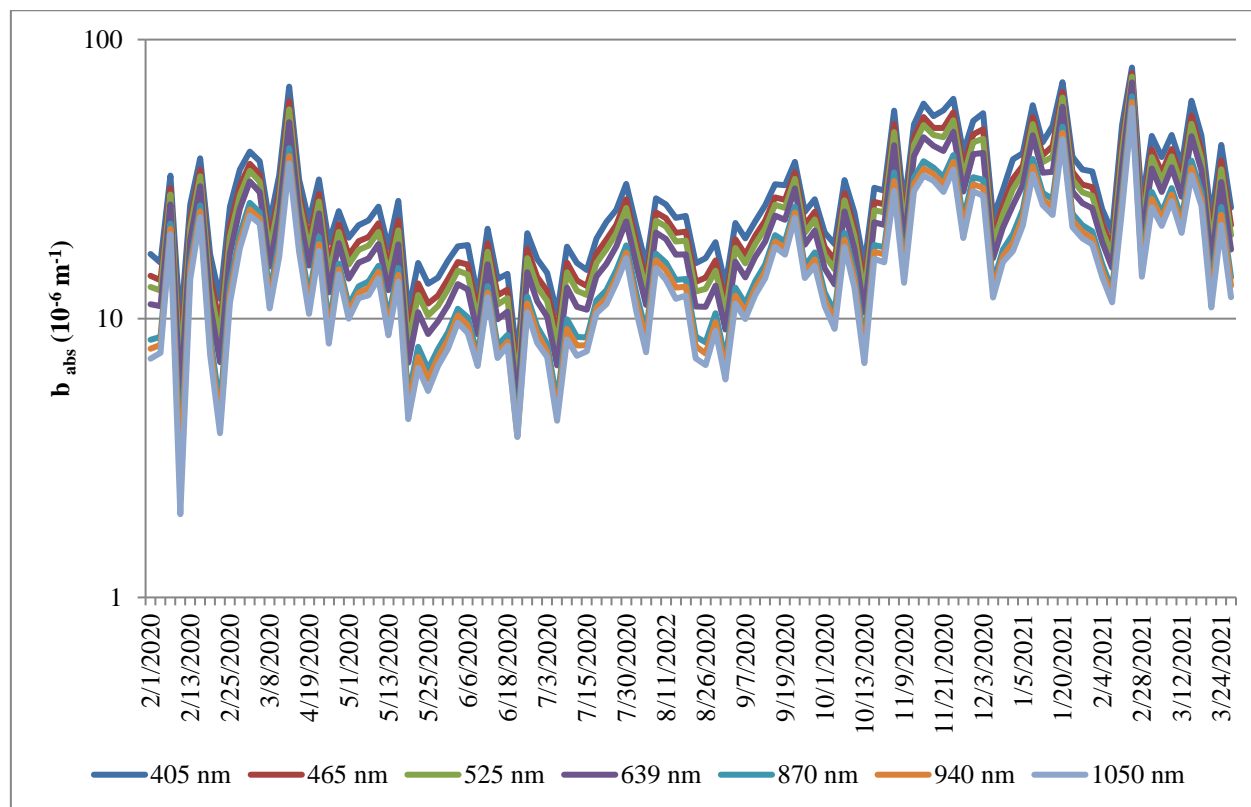
117 where  $a$  and  $\alpha$  are constants.



118

119 **Figure 2** The mass absorption coefficient ( $\epsilon$ ) versus wavelength ( $\lambda$ ) obtained for sampling from the Krakow site.

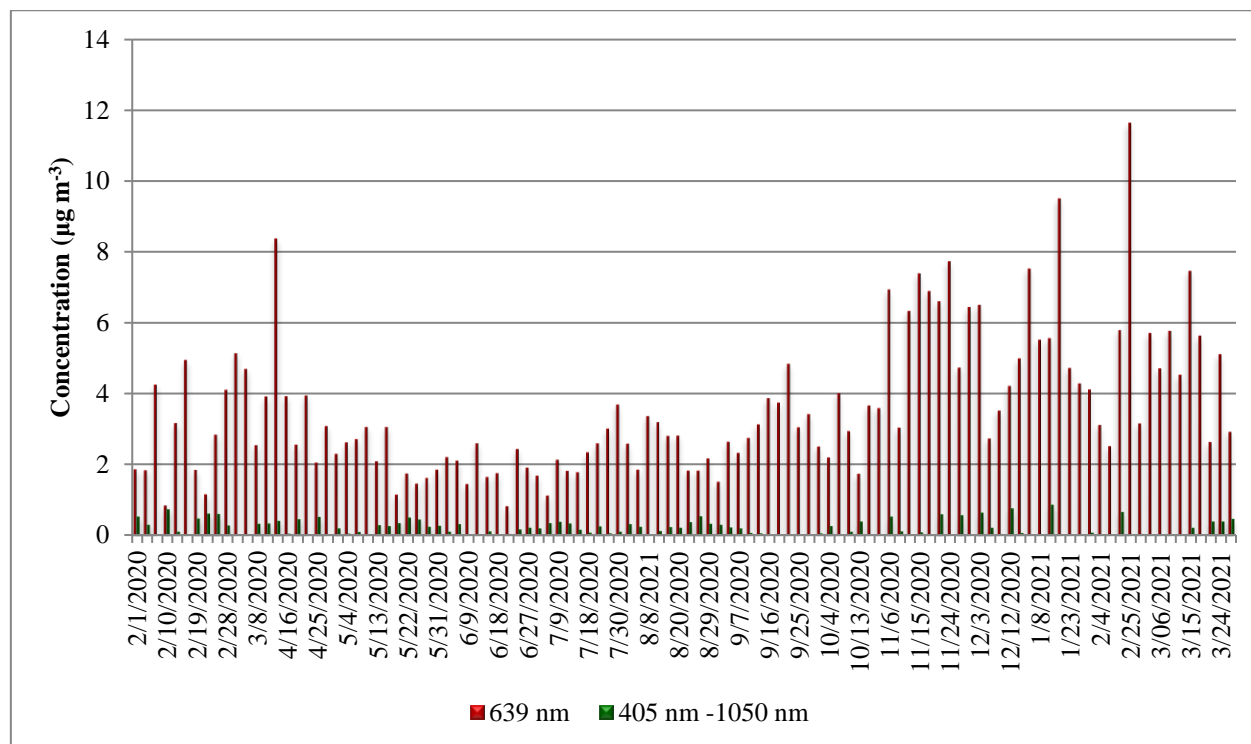
120 Figure 2 shows the mass absorption coefficient values for each wavelength. The fitted coefficient were:  $a = 285.3$  and  $\alpha =$   
121  $0.599$ . “This value of  $\alpha$  lower than unity implies that the BC particles we generally measure have core diameters in the range  
122  $150 \text{ nm}$  to  $200 \text{ nm}$ ” (David D. Cohen, 2020). The correlation was very strong with power dependence and coefficient of least  
123 squares  $R^2 > 0.99$ . The shape of the fit curve is as expected and mass absorption coefficient values fall within the range of 4-  
124  $11 \text{ m}^2 \text{ g}^{-1}$  which is consistent with the recommendations (Atanacio et al., n.d.).



125

126 **Figure 3 The light absorption coefficients ( $b_{\text{abs}}$ ) at seven wavelength (nm) for sampling from Krakow during February 2020 – March**  
127 **2021 in  $10^{-6} \text{ m}^{-1}$ .**

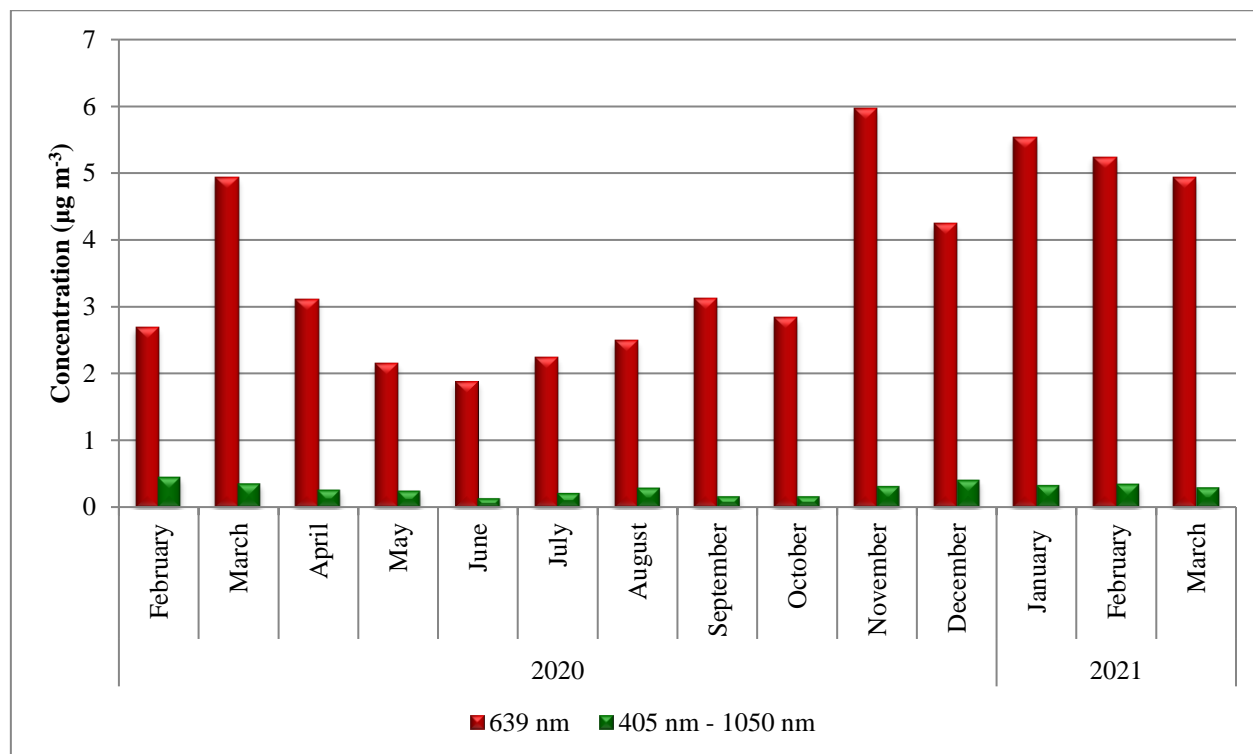
128 In Figure 3, the black carbon light ( $b_{\text{abs}}$ ) fluctuated during the whole sampling time. The big differences, between February,  
129 March, November, December and June-July periods, suggest that during the cold season there was increased emission of BC  
130 for instance from combustion in a residential area, which was expected. During May, June and July, ( $b_{\text{abs}}$ ) have smaller and  
131 more stable values. The shape of the curve and values for absorption coefficients ( $b_{\text{abs}}$ ) can be compared to the research from  
132 Greece 2017 (Diapouli et al., 2017).



133

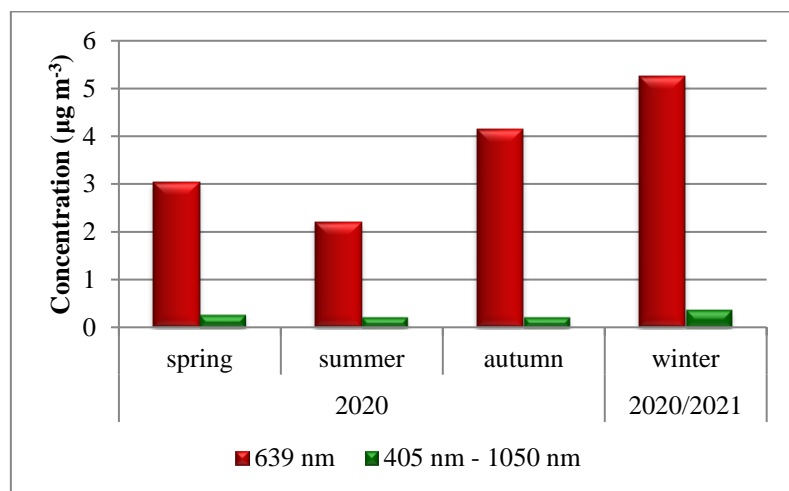
134 **Figure 4 Comparison daily concentrations between eBC for 639 nm and BC for (405nm – 1050nm) in  $\mu\text{g m}^{-3}$  for sampling from**  
135 **Krakow during February 2020 – March 2021.**

136 The red curve, in Figure 4, is the equivalent black estimate from MABI using 639 nm data. These data include, among other,  
137 smoke components, diesel, fossil fuels, etc. The values obtained by subtracting the BC (1050 nm) data from BC (450 nm) data,  
138 the green curve, represent mainly BC from biomass burning. It was expected that there are no significant biomass burning  
139 event and increased pollution came from fossil fuels and transport. However, the values of BC from biomass burning were  
140 similar to values obtained by Christian et al. in Calaca where mean values were  
141  $0.67 \mu\text{g m}^{-3}$  for winter 2019 (Duc et al., 2020; Tusó et al., 2020). It can be seen in Figure 4 and Figure 5, that the values of BC  
142 increased during March (2020, 2021), November, December (2020) and February (2021), but at May, June, July was lower and  
143 this was the expected effect of emission from combustion. Especially, in the cold season, also there were days when the values  
144 for eBC were particularly high. It can be explained as following, during the cold period, there is the increase of utilization the  
145 fossil fuels among other to a heating household of coal also it can see increased traffic. Moreover, the windless weather and  
146 low temperature are responsible for the lack of air movement and the accumulation of pollution in one place. Which causes an  
147 increase in the concentration of  $\text{PM}_{2.5}$  and eBC in the city. Interestingly, the low values of concentration BC for February 2020,  
148 had confirmed in low concentration  $\text{PM}_{2.5}$ , what can suggest better weather condition compared to February 2021.  
149 The exposed filter from 25 February 2021 (25-02-2021 in Figure 4 and Figure 8) was the blackest which is visually evident  
150 when is compared with all exposed filters and this is a confirmation of the highest values eBC for the peak from the day.



151

152 **Figure 5** Mean monthly concentrations of eBC for 639 nm and BC for (405nm – 1050nm) in  $\mu\text{g m}^{-3}$  for sampling from Krakow  
153 during 2020 – 2021.



154

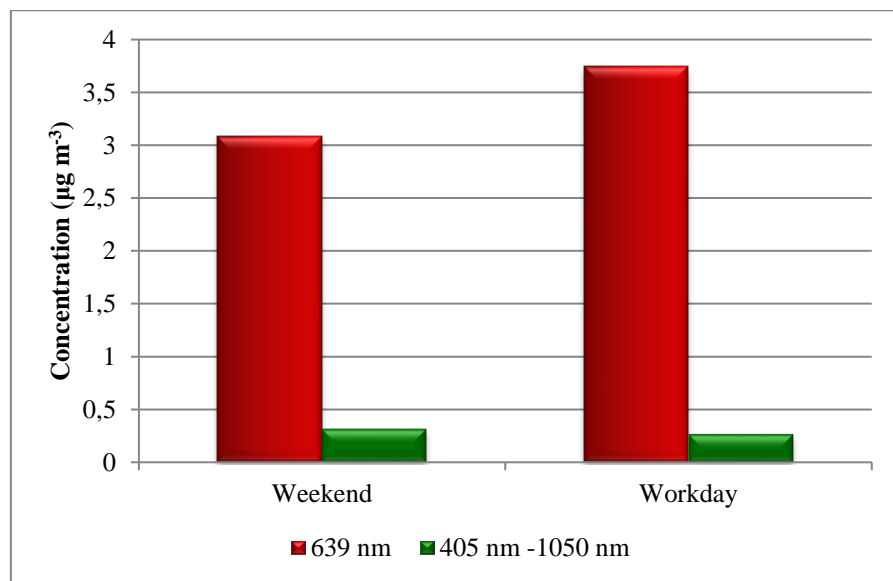
155 **Figure 6** Seasonal concentrations of eBC for 639 nm and BC for (405 nm – 1050nm) in  $\mu\text{g m}^{-3}$ .

156 The Figure 6 presents seasonal concentration, where seasons consist of: spring - March, April, May (2020); summer - June,  
157 July, August (2020); autumn - September, October, November(2020); winter - December(2020), January, February(2021).

158 The mean values of eBC concentration are the highest for winter, and the lowest for summer, which was the expected outcome.



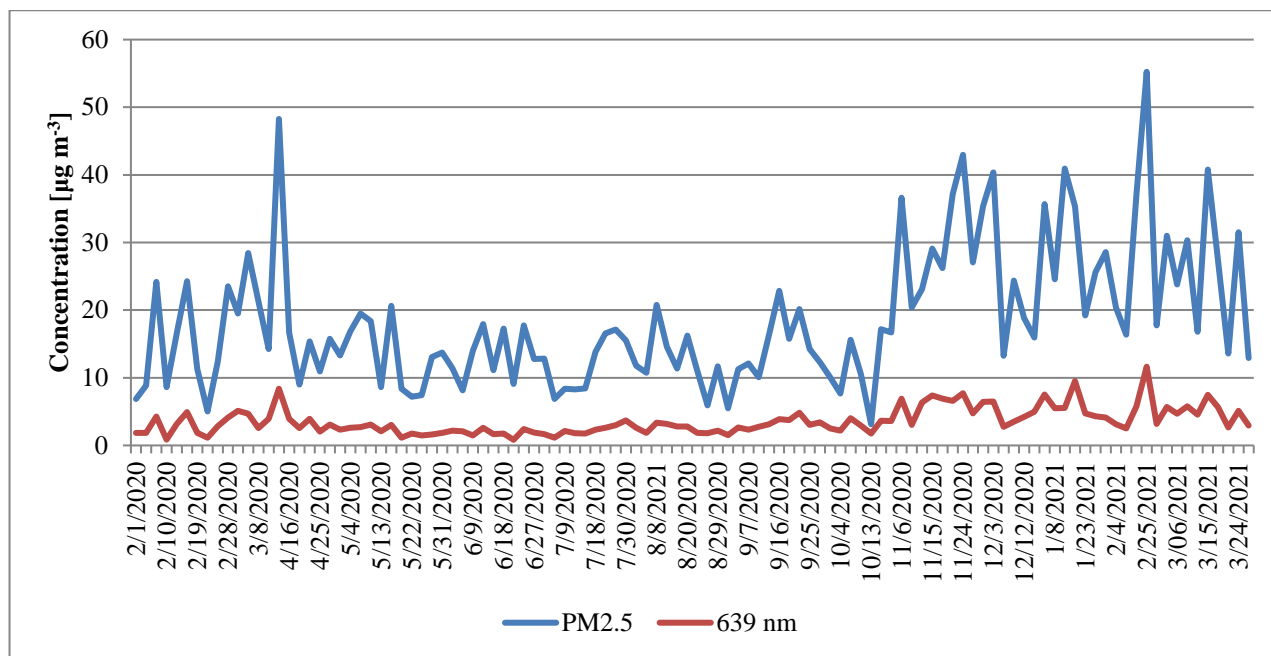
159 The values concentrations of BC for (405 nm – 1050 nm) can be considered constant for all seasons, which can be in connection  
160 with biomass burning like wood etc in a household to heating water, in fireplace etc. The low value of BC for biomass and ban  
161 of burning coal and wood in Krakow can suggested that this pollution could come not only from Krakow, but also from  
162 neighbourhood towns which used biomass to heat the houses, heat the water etc.



163

164 **Figure 7 Mean concentrations of eBC for 639 nm and BC for (405nm – 1050nm) for weekend and workdays**

165 Based on Figure 7, it can be seen that the concentration of eBC was higher for workdays than weekends. It can be in connection  
166 with more intense traffic during workdays than at weekends. There was no significant difference between workdays and  
167 weekends in terms of BC for (405 nm - 1050 nm).



168

169 **Figure 8 Daily concentrations of PM<sub>2.5</sub> and eBC µg m<sup>-3</sup>.**

170 Figure 8 presents the daily concentrations of PM<sub>2.5</sub> and eBC. As can be seen, it covers 14 months. It can be seen, that with the  
 171 concentration of the values PM<sub>2.5</sub> growth eBC was increasing and if values of PM<sub>2.5</sub> dropped then eBC (639nm) dropped too,  
 172 especially during the cold period (November, December, January, February, March). However, the concentration of PM<sub>2.5</sub> had  
 173 lower values in May, June, July, which was the expected effect of lower emission from combustion (also in Figure 5). In this  
 174 season, the values of eBC were more stable and seem to be kept constant despite the pick of PM<sub>2.5</sub> has fluctuated, which proves  
 175 that the sources of pollution were not only combustion and traffic.

176 Based on Table 1, it can be seen that if the PM<sub>2.5</sub> concentration was higher consequently the concentration of eBC was also  
 177 higher. In winter the values of PM<sub>2.5</sub> and eBC were picked in comparison to other seasons, and the values in summer were the  
 178 lowest what was expected.

179 **Table 1 Mean concentrations of PM<sub>2.5</sub>, equivalent black carbon, black carbon related to biomass (BC<sub>BB</sub>) in µg m<sup>-3</sup> with standard**  
 180 **deviation, and relative contribution of biomass (BC<sub>BB</sub>) to eBC in % for the season, year and full sampling period.**

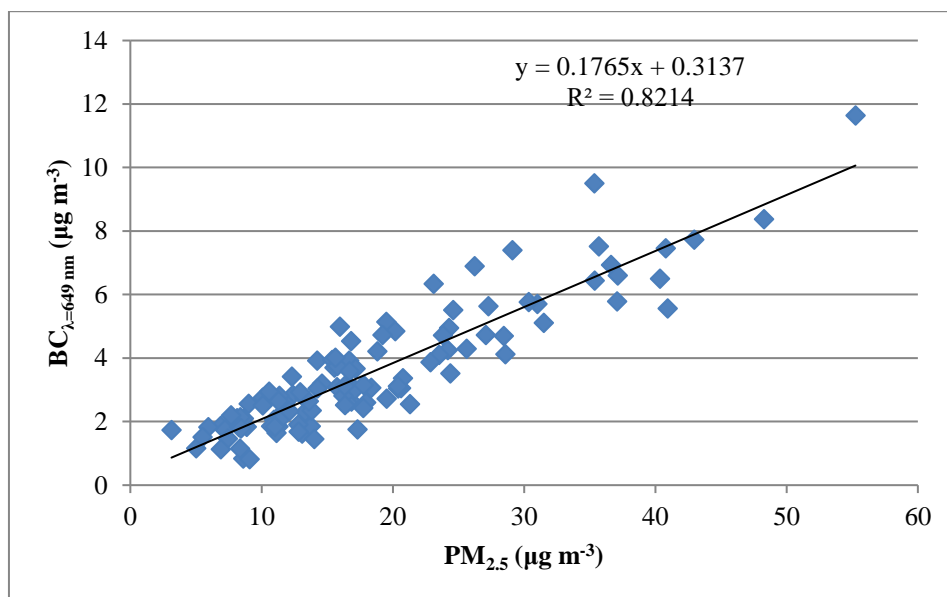
PERIOD	PM <sub>2.5</sub> (µg m <sup>-3</sup> )	eBC (µg m <sup>-3</sup> )	BC <sub>BB</sub> (µg m <sup>-3</sup> )	BC <sub>BB</sub> /eBC (%)
Spring	16.5 ± 0.2	3.0 ± 1.1	0.3 ± 0.1	12.3 ± 8.2
Summer	12.6 ± 0.1	2.2 ± 0.5	0.2 ± 0.1	10.8 ± 6.0
Autumn	19.2 ± 0.7	4.2 ± 1.6	0.22 ± 0.16	7.0 ± 5.1
Winter	27.6 ± 0.2	5.3 ± 1.8	0.4 ± 0.3	6.7 ± 5.5
Annual	18.2 ± 0.6	3.5 ± 1.5	0.25 ± 0.15	9.7 ± 6.5
Full period	18.4 ± 0.6	3.6 ± 1.5	0.3 ± 0.2	11.3 ± 8.4



181 In Table 1, the eBC represents the values of concentration ( $\mu\text{g m}^{-3}$ ) which were obtained for  $\lambda = 639$  nm; the  $\text{BC}_{\text{BB}}$  - the values  
182 were obtained for  $\lambda = 405$  nm-1050 nm. The annual period of mean sampling was from March 2020 to February 2021, and the  
183 full period – February 2020 to March 2021. It can be seen, that  $\text{BC}_{\text{BB}}$  has higher values in winter than summer and autumn  
184 which was connected with increased emission from combustion in the cold period. It can be expected, that percentage of  $\text{BC}_{\text{BB}}$   
185 could be higher in winter.

186 The values for eBC which were obtained in this study were similar to the result from the previous study presented among other  
187 by Cruz et al. which was carried out during one year in 2018 and by Reche et al. in 2009 (Cruz et al., 2019; Reche et al., 2011;  
188 Stahl et al., 2020).

189 Moreover, in this study, eBC was reported for 639 as is suggested by Atanacio et al. (Atanacio et al., n.d.). The analysis, which  
190 is presented in Figure 9, shows the relationship between eBC and  $\text{PM}_{2.5}$ , which was confirmed by a strong correlation. Based  
191 on this graph, it can be concluded, that about 18 % of  $\text{PM}_{2.5}$  mass belongs to eBC. Similar event were also observed in other  
192 studies where the ratio  $\text{BC}/\text{PM}_{2.5}$  was about among the other 21 % and 13 % in Liverpool and Newcastle, respectively (Cohen  
193 et al., 2000; Duc et al., 2020).



194  
195 **Figure 9 Regression of concentration eBC for  $\lambda = 639$  nm versus  $\text{PM}_{2.5}$  for full period.**

#### 196 **4 Conclusion**

197 To develop a strategy for lowering the concentration of black carbon in air particulate matter it is crucial to determine its  
198 sources first. The optical absorption method allows assessing concentrations of equivalent black carbon together with the  
199 contribution of different sources to eBC. The present study describes the methodology for the determination of eBC  
200 concentrations and assesses the contribution of sources like fossil fuel/traffic and biomass burning to  $\text{PM}_{2.5}$  mass. What is



201 more, we present the result with an extensive analysis of the annual period. Our work proves that fossil fuel/traffic contribution  
202 to  $PM_{2.5}$  mass is higher in winter than in warm seasons. The contribution of fossil fuel/traffic is higher than biomass burning  
203 during the whole sampling period. Moreover, the concentrations of eBC and biomass burning were more stable during May,  
204 June, July than in the cold period.

#### 205 **Author contribution**

206 AR and LS planned the experiment. AR collected samples and performed measurements and calculation. AR and LS made  
207 interpretation data, write manuscript. Both authors contributed to the paper discussion and revision.

#### 208 **Competing interests**

209 "The authors declare no conflict of interest".

#### 210 **Acknowledgements**

211 The International Atomic Energy Agency, project number RER/7/012 partially financed this work together with the subsidy  
212 of the Ministry of Science and Higher Education, grant number 16.16.220.842.

213 Research project supported/partly supported by program "Excellence initiative – research university" for the University of  
214 Science and Technology.

215



## 216 References

- 217 Atanacio, A. J., Cohen, D. D., Button, D., Paneras, N. and Garton, D.: Multi-wavelength Absorption Black Carbon Instrument  
218 ( MABI ) Manual., n.d.
- 219 Bond, T. C. and Bergstrom, R. W.: Light Absorption by Carbonaceous Particles: An Investigative Review, *Aerosol Sci.*  
220 *Technol.*, 40(1), 27–67, <https://doi.org/10.1080/02786820500421521>, 2006.
- 221 Cohen, D. D., Taha, G., Stelcer, E., Garton, D. and Box, G.: The Measurement and Sources of Fine Particle Elemental Carbon  
222 at Several Key Sites in NSW over the Past Eight Years ., in 15th International Clean Air Conference, pp. 485–490, , 2000.
- 223 Cruz, M. T., Cruz, M. T., Bañaga, P. A., Betito, G., Braun, R. A., Stahl, C., Aghdam, M. A., Obiminda Cambaliza, M.,  
224 Dadashazar, H., Hilario, M. R., Lorenzo, G. R., Ma, L., MacDonald, A. B., Pabroa, P. C., Yee, J. R., Simpas, J. B. and  
225 Sorooshian, A.: Size-resolved composition and morphology of particulate matter during the southwest monsoon in Metro  
226 Manila, Philippines, *Atmos. Chem. Phys.*, 19(16), 10675–10696, <https://doi.org/10.5194/acp-19-10675-2019>, 2019.
- 227 David D. Cohen: Summary of Light Absorbing Carbon and Visibility Measurements and Terms. ANSTO External Report ER-  
228 790, ISBN – 1 921268 32 8, October 2020., 2020.
- 229 Diapouli, E., Kalogridis, A. C., Markantonaki, C., Vratolis, S., Fetfatzis, P., Colombi, C. and Eleftheriadis, K.: Annual  
230 variability of black carbon concentrations originating from biomass and fossil fuel combustion for the suburban aerosol in  
231 Athens, Greece, *Atmosphere (Basel)*., 8(12), <https://doi.org/10.3390/atmos8120234>, 2017.
- 232 Duc, H. N., Shingles, K., White, S., Salter, D., Chang, L. -C. ., Gunashanhar, G., Riley, M., Trieu, T., Dutt, U., Merched;, A.,  
233 Beyer, K., Hynes, R. and Kirkwood, J.: Spatial-Temporal Pattern of Black Carbon (BC) Emission from Biomass Burning and  
234 Anthropogenic Sources in New South Wales and the Greater Metropolitan Region of Sydney, Australia, *Atmosphere (Basel)*.,  
235 11, 570, <https://doi.org/10.3390/atmos11060570>, 2020.
- 236 European Environment Agency: Status of black carbon monitoring in ambient air in Europe., 2013.
- 237 Horvath, H.: Atmospheric light absorption—A review, *Atmos. Environ. Part A. Gen. Top.*, 27(3), 293–317,  
238 [https://doi.org/https://doi.org/10.1016/0960-1686\(93\)90104-7](https://doi.org/https://doi.org/10.1016/0960-1686(93)90104-7), 1993.
- 239 Jacobson, M. Z.: Strong radiative heating due to the mixing state of black carbon in atmospheric aerosols, *Nature*, 409(6821),  
240 695–697, <https://doi.org/10.1038/35055518>, 2001.
- 241 Lack, D., Moosmuller, H., McMeeking, G., Chakrabarty, R. and Baumgardner, D.: Characterizing elemental, equivalent black,  
242 and refractory black carbon aerosol particles: A review of techniques, their limitations and uncertainties, *Anal. Bioanal. Chem.*,  
243 406, <https://doi.org/10.1007/s00216-013-7402-3>, 2013.
- 244 Liu, Q., Ma, T., Olson, M. R., Liu, Y., Zhang, T., Wu, Y. and Schauer, J. J.: Temporal variations of black carbon during haze  
245 and non-haze days in Beijing, *Sci. Rep.*, 6(1), 33331, <https://doi.org/10.1038/srep33331>, 2016.
- 246 Petzold, A. and Schönlinner, M.: Multi-angle absorption photometry—a new method for the measurement of aerosol light  
247 absorption and atmospheric black carbon, *J. Aerosol Sci.*, 35(4), 421–441,  
248 <https://doi.org/https://doi.org/10.1016/j.jaerosci.2003.09.005>, 2004.



- 249 Petzold, A., Ogren, J. A., Fiebig, M., Laj, P., Li, S. M., Baltensperger, U., Holzer-Popp, T., Kinne, S., Pappalardo, G.,  
250 Sugimoto, N., Wehrli, C., Wiedensohler, A. and Zhang, X. Y.: Recommendations for reporting black carbon measurements,  
251 *Atmos. Chem. Phys.*, 13(16), 8365–8379, <https://doi.org/10.5194/acp-13-8365-2013>, 2013.
- 252 Reche, C., Querol, X., Alastuey, A., Viana, M., Pey, J., Moreno, T., Rodr\`iguez, S., González, Y., Fernández-Camacho, R.,  
253 de la Rosa, J., Dall’Osto, M., Prévôt, A. S. H., Hueglin, C., Harrison, R. M. and Quincey, P.: New considerations for PM,  
254 Black Carbon and particle number concentration for air quality monitoring across different European cities, *Atmos. Chem.*  
255 *Phys.*, 11(13), 6207–6227, <https://doi.org/10.5194/acp-11-6207-2011>, 2011.
- 256 Stahl, C., Cruz, M. T., Bañaga, P. A., Betito, G., Braun, R. A., Aghdam, M. A., Cambaliza, M. O., Lorenzo, G. R., MacDonald,  
257 A. B., Pabroa, P. C., Yee, J. R., Simpas, J. B. and Sorooshian, A.: An annual time series of weekly size-resolved aerosol  
258 properties in the megacity of Metro Manila, Philippines, *Sci. Data*, 7(1), 128, <https://doi.org/10.1038/s41597-020-0466-y>,  
259 2020.
- 260 Taha, G., Box, G. P., Cohen, D. D. and Stelcer, E.: Black Carbon Measurement using Laser Integrating Plate Method, *Aerosol*  
261 *Sci. Technol.*, 41(3), 266–276, <https://doi.org/10.1080/02786820601156224>, 2007a.
- 262 Taha, G., Box, G., Cohen, D. and Stelcer, E.: Black Carbon Measurement using Laser Integrating Plate Method, *Aerosol Sci.*  
263 *Technol. - AEROSOL SCI TECH*, 41, 266–276, <https://doi.org/10.1080/02786820601156224>, 2007b.
- 264 Tuso, C. A. T., Magtaas, R. A. H., Punzalan, J. M., Yee, J. R., Bautista, A. T. and Pabroa, P. C. B.: Air particulate matter,  
265 black carbon, and elemental concentrations and source apportionment in Calaca, Batangas, *Philipp. J. Sci.*, 149(Special Issue  
266 1), 117–127, 2020.
- 267 U.S. EPA (U.S. Environmental Protection Agency): Report to Congress on Black Carbon., 2012.